Reproducibility of 3′-Deoxy-3′-^{18}F-Fluorothymidine MicroPET Studies in Tumor Xenografts in Mice

Jeffrey R. Tseng, MD[1]; Mangal Dandekar, MS[1]; Murugesan Subbarayan, PhD[1]; Zhen Cheng, PhD[1]; Jinha M. Park, MD, PhD[1,2]; Stan Louie, PharmD, PhD[3]; and Sanjiv S. Gambhir, MD, PhD[1]

[1]Molecular Imaging Program of Stanford, Bio-X Program, and Department of Radiology, Stanford University School of Medicine, Stanford, California; [2]Department of Radiology, University of California, Los Angeles, Los Angeles, California; and [3]Department of Pharmacy, University of Southern California, Los Angeles, California

3′-Deoxy-3′-^{18}F-fluorothymidine (^{18}F-FLT) has been used to image tumor proliferation in preclinical and clinical studies. Serial microPET studies may be useful for monitoring therapy response or for drug screening; however, the reproducibility of serial scans has not been determined. The purpose of this study was to determine the reproducibility of ^{18}F-FLT microPET studies. **Methods:** C6 rat glioma xenografts were implanted into nude mice (n = 9) and grown to mean diameters of 5–17 mm for approximately 2 wk. A 10-min acquisition was performed on a microPET scanner approximately 1 h after ^{18}F-FLT (1.9–7.4 MBq [50–200 μCi]) was injected via the tail vein. A second microPET scan was performed approximately 6 h later on the same day after reinjection of ^{18}F-FLT to assess for reproducibility. Most of the mice were studied twice within the same week (for a total of 17 studies). Images were analyzed by drawing an ellipsoidal region of interest (ROI) around the tumor xenograft activity. Percentage injected dose per gram (%ID/g) values were calculated from the mean activity in the ROIs. Coefficients of variation and differences in %ID/g values between studies from the same day were calculated to determine the reproducibility after subtraction of the estimated residual tumor activity from the first ^{18}F-FLT injection. **Results:** The coefficient of variation (mean ± SD) for %ID/g values between ^{18}F-FLT microPET scans performed 6 h apart on the same day was 14% ± 10%. The difference in %ID/g values between scans was −0.06% ± 1.3%. Serum thymidine levels were mildly correlated with %ID/g values (R^2 = 0.40). Tumor size, mouse body weight, injected dose, and fasting state did not contribute to the variability of the scans; however, consistent scanning parameters were necessary to ensure accurate studies, in particular, controlling body temperature, the time of imaging after injection, and the ROI size. **Conclusion:** ^{18}F-FLT microPET mouse tumor xenograft studies are reproducible with moderately low variability. Serial studies may be performed to assess for significant changes in therapy response or for preclinical drug development.

Received May 11, 2005; revision accepted Aug. 1, 2005.

For correspondence or reprints contact: Sanjiv S. Gambhir, MD, PhD, Molecular Imaging Program at Stanford, Bio-X Program, and Department of Radiology, The James H. Clark Center, 318 Campus Dr., East Wing, 1st Floor, Stanford, CA 94305-5427.

E-mail: sgambhir@stanford.edu

Key Words: ^{18}F-FLT; microPET; reproducibility; tumor xenograft; drug development

J Nucl Med 2005; 46:1851–1857

The radioactive thymidine analog 3′-deoxy-3′-^{18}F-fluorothymidine (^{18}F-FLT) has been used to assess tumor proliferation (*1*) as a reflection of mammalian thymidine kinase activity (*2–5*). In clinical studies, ^{18}F-FLT has been used for the diagnosis and staging of lung cancer, colon cancer, breast cancer, melanoma, sarcoma, laryngeal cancer, and lymphoma (*6–13*); however, some studies have shown that the sensitivity of ^{18}F-FLT is lower than that of ^{18}F-2′-fluoro-2′-deoxyglucose (^{18}F-FDG).

An important developing application for ^{18}F-FLT is assessing tumor response to therapy. Inhibition of tumor proliferation may be an early marker for response to therapy, as shown in microPET animal tumor xenograft studies (*14–17*), and may lead to earlier treatment decisions. For assessment of therapy response, serial studies must be performed to track changes in activity over time, usually within days to weeks. The scans must be reproducible so that serial changes reflect therapy effects rather than changes attributable to variabilities in the methodology or mouse physiology. In addition to assessing therapy response, serial microPET studies can be performed in the preclinical drug screening process during drug development. Lead candidate drugs may be rapidly assessed for their ability to inhibit tumor proliferation as a marker of drug efficacy.

Two studies have been conducted to assess the reproducibility of PET with ^{18}F-FDG in human cancer studies (*18,19*). These studies showed that the variation across serial scans was approximately 6%–10%, on the basis of an analysis of the standardized uptake value (SUV) or kinetic modeling parameters. With the increased use of microPET studies with ^{18}F-FLT, particularly for therapy monitoring, reproducibility needs to be well documented. The purpose of this study was to determine the reproducibility of microPET studies with ^{18}F-

FLT in a mouse tumor xenograft model. We show that the reproducibility has moderately low variability, which will allow for serial drug or therapy evaluations.

MATERIALS AND METHODS

Radiotracers

^{18}F-FLT was prepared by reaction of no-carrier-added ^{18}F-fluoride (PETNET Pharmaceuticals) with the precursor, 5′-*O*-benzoyl-2,3′-anhydrothymidine, and then 1% NaOH hydrolysis (*20*) in a TRACERlab FxFN automatic synthesis module (General Electric). The typical yield was 10%–15% (decay corrected), and the specific activity was >45 TBq/mmol. [Methyl-^{3}H(*N*)]-3-deoxy-3-fluorothymidine (^{3}H-FLT) was purchased from Moravek Biochemicals and had a specific activity of 130 GBq/mmol.

C6 Cell Cultures

C6 rat glioma cells were grown in Dulbecco modified Eagle medium with high concentrations of glucose and L-glutamine (Invitrogen) and supplemented with 10% fetal bovine serum and penicillin (100 U/mL)–streptomycin (100 μg/mL). Cells were harvested by trypsinization at approximately 90% confluence. C6 cells showed linear ^{18}F-FLT accumulation in vitro over 2 h, with 6.3% accumulation being reached at 2 h (data not shown); these results were similar to results obtained with pancreatic cell lines by Seitz et al. (*3*).

Thymidine–^{3}H-FLT Competition Assay in C6 Cells

Triplicate samples of 5×10^5 C6 cells were plated on 12-well plates and grown overnight in 1 mL of medium. Various concentrations of thymidine (Sigma) (100 pg/mL–100 μg/mL) were added. ^{3}H-FLT at 0.037 MBq (1 μCi) was added to each well and incubated at 37°C for 90 min. Cells were rinsed 3 times with 1 mL of cold phosphate-buffered saline and then lysed with 300 μL of 1N NaOH. Radioactivity was counted by use of an LS 6500 scintillation counter (Beckman Coulter) with Bio-Safe II scintillation fluid (Research Products International). Total protein was determined for each well (protein assay; Bio-Rad Laboratories) and used to normalize the activity measurements. Activity versus log thymidine concentration was plotted, and the 50% inhibitory concentration was determined by graphical estimation.

Mouse Serum Thymidine Analysis

Retro-orbital blood samples (approximately 200 μL) were obtained from 6 mice after the second scan (6 h after the first scan). Blood was allowed to coagulate at room temperature for 1 h and then centrifuged at 2,300*g* in a Microcentrifuge 5415D (Eppendorf). Serum was separated from the blood cells and stored at −80°C until analysis.

Fifty microliters of carbovir dissolved in methanol (500 ng/mL) and in 500 μL of acetonitrile (to precipitate proteins) was added to 50-μL mouse serum samples and then centrifuged at 18,000*g* for 5 min. The supernatants were aspirated and then evaporated to dryness under a steady stream of filtered air at room temperature. The residuals were reconstituted with 150 μL of 0.1% formic acid and then centrifuged at 18,000*g* for 5 min.

Serum thymidine levels were determined by use of liquid chromatography–tandem mass spectrometry (LC-MS/MS). A 20-μL sample was injected into an Agilent 1100 quaternary high-performance liquid chromatography system (Agilent Technologies) fitted with an ACE C_{18} column (2 × 50 mm, 5 μm packing; Thermo Electron Corp.). The mobile phase consisted of 15% (v/v) methanol and 85% (v/v) 0.1% formic acid. The flow rate was 0.3 mL/min. The eluents were quantified by use of a triple–quadrupole mass spectrometry system (API 3+; MDS Sciex) in the positive mode with a turbo–ion-spray source. The mass transitions were 243→127 and 248→152, and the retention times were 2.1 and 3.2 min for thymidine and carbovir, respectively. A linear calibration standard was prepared with thymidine concentrations of 25–2,000 ng/mL in mouse serum; the interday precision and accuracy coefficients of variation ranged from 1.8% to 6.9%, and the error rates ranged from −6.7% to 6.1%.

Mouse Tumor Xenograft Model

Animal protocols were approved by the Stanford Administrative Panel on Laboratory Animal Care. Nine female nude mice (Charles River Laboratories, Inc.) were injected in the shoulder region with 10^6 C6 cells in 100 μL of phosphate-buffered saline by use of 28G1/2 insulin syringes (Becton Dickinson). The mice were anesthetized with 2% isoflurane in oxygen at 2 L/min during the injections. The tumor xenografts grew for 1–2 wk, until the mean diameters were 5–17 mm (volume, 65–2,500 mm^3). A minimum of 5 mm was chosen to avoid partial-volume effects (*21*). Three mice were excluded from the analysis because their body temperature during the first uptake and scan period was 24°C. A subanalysis was performed on these mice to assess the effects of body temperature on ^{18}F-FLT accumulation.

microPET Imaging

An R4 microPET system (Concorde Microsystems Inc.) was used for imaging; this system has an approximate resolution of 2 mm in each axial direction (*22*). At approximately 60 min after a tail vein injection of ^{18}F-FLT at 1.9–7.4 MBq (50–200 μCi), a 10-min prone acquisition scan was performed. Mice were maintained under isoflurane anesthesia during the entire uptake and scanning periods. A heating pad or heat lamp was used to maintain body temperatures at about 35°C. A second scan was performed with a repeat injection of ^{18}F-FLT at approximately 6 h after the first injection. Six hours was chosen to allow the activity from the first injection to decay for approximately 3 half-lives. It was assumed that the tumor xenografts did not significantly change during the 6 h. Caliper tumor measurements were not significantly different between the 2 scans. Most mice were studied twice within the same week (for a total of 17 studies). Mouse body weight and temperature were recorded. Approximately half of the studies were performed with a 4-h fast before injection ($n = 8$), and the remaining studies were performed without a fast ($n = 9$). Five mice were scanned at 4 h after the first injection to assess the change in activity over time. The mouse tails were curled cephalad so that they were included in the microPET field of view to allow assessment of radiotracer infiltration in the tail because of a difficult tail vein injection.

microPET images were reconstructed by use of the ordered-subsets expectation maximization algorithm (*23*) with 12 subsets and 4 iterations. No attenuation correction was applied, because an attenuation-corrected cylinder phantom study and an attenuation correction scan performed with the body outline of a mouse with uniform attenuation both showed very little change in the activity profile across the mouse.

microPET Image Analysis

Ellipsoidal three-dimensional (3D) regions of interest (ROIs) were manually drawn around the edge of the tumor xenograft activity by visual inspection with AMIDE software (Andreas Loen-

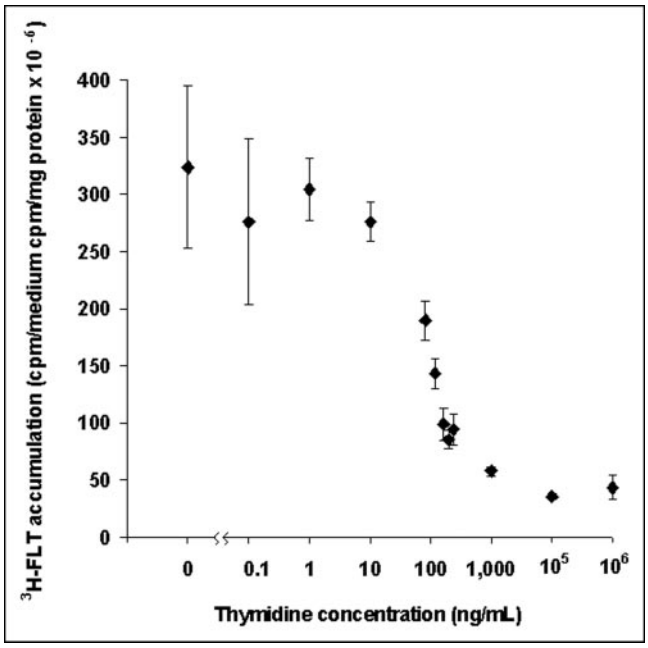

FIGURE 1. Competition between various concentrations of thymidine and ^{3}H-FLT in C6 rat glioma cells. Accumulation values represent tracer activity relative to activity in medium, normalized to total protein. Thymidine concentrations are plotted on log scale. Error bars represent 1 SD for triplicate samples.

ing; available at http://amide.sourceforge.net/) (*24*). The mean and maximum activities were recorded from the entire ROI. The percentage injected dose per gram (%ID/g) and the SUV were calculated as follows: %ID/g = ROI activity divided by injected dose; SUV = (ROI activity times body weight) divided by injected dose. Activity in the second scan, at 6 h, was adjusted by subtracting the decay-corrected activity of the first scan. Differences between the first scan and the second scan were calculated. The coefficient of variation (CV) was calculated as the SD of the first scan and second scan divided by their mean. CV has been used as a statistical measure of absolute reliability (*25*). The intraclass correlation coefficient also was calculated.

To assess the variability of ROI placement, ROIs were redrawn around the tumors 2 mo later on a subset of 10 studies by the original analyzer and by a second analyzer. The analyzers redrew ROIs in 1 analysis. In a second analysis, ROIs that were the same sizes as the original ROIs were placed. CVs were recalculated for the ROI sizes and the mean %ID/g values.

Statistical Analysis

Statistical analysis was performed with Excel 2002 (Microsoft) and Statview version 5.0.1 (SAS Institute) software. Paired *t* tests were used when paired data from the same mouse were compared. Unpaired *t* tests were used when 2 groups of data were compared. Correlation coefficients were calculated when 2 groups of nominal variables were compared. A significance value of $P < 0.05$ was used. Data are reported as mean ± SD.

RESULTS

Thymidine Levels

C6 cells were incubated with various concentrations of thymidine to assess for competition with ^{3}H-FLT accumulation. The plot of activity versus log thymidine concentration (Fig. 1) revealed a monophasic competition curve with a 50% inhibitory concentration of 90 ng/mL.

Serum thymidine levels were determined in 6 mice and compared with %ID/g values determined by microPET. A mild inverse correlation between serum thymidine levels and ^{18}F-FLT accumulation (%ID/g) was seen (Fig. 2). The serum thymidine values varied widely, with a range of 107–411 ng/dL and a mean ± SD of 289 ± 107 ng/dL.

^{18}F-FLT microPET Studies of Mouse Tumor Xenografts

Tumor xenografts were clearly visible on the microPET images of all mice (mean ± SD diameter, 10.6 ± 4.3 mm; range, 4.9–17.2 mm). The peripheries of the tumors were easily delineated for ROI placement on the images. The mean diameters of the ROIs drawn around the tumor activity correlated well with the mean caliper measurements of the tumors ($R^2 = 0.94$; slope of linear fit, 1.07). Several tumors exhibited more intense activity at their peripheries, suggesting a higher level of proliferation (Fig. 3).

Five mice were scanned at 4 h after tail vein injection of ^{18}F-FLT (Fig. 4) to assess the change in activity over time. The %ID/g increased for 3 mice (52% ± 41%) and decreased for 2 mice (−50% ± 11%). The mean ± SD tumor-to-background ratio (background is the ROI around the adjacent thorax) increased from 1.8 ± 1.1 to 7.3 ± 6.9 ($P = 0.04$), a 3-fold increase over 3 h. These data suggest that for lesions difficult to visualize on early scanning at 1 h, delayed imaging may be helpful. Bone marrow activity was not visible on any scans at 1 h; however, bone marrow activity was seen on 2 of the 5 delayed scans. This finding

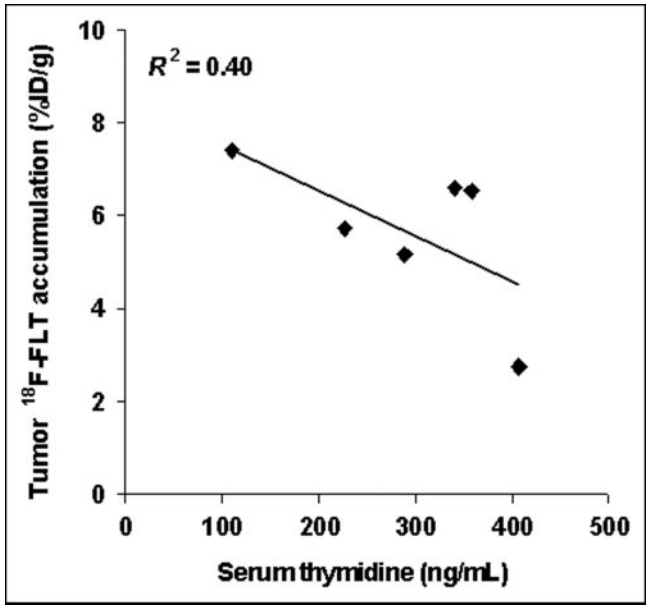

FIGURE 2. Correlation between mouse serum thymidine levels determined by LC-MS/MS and ^{18}F-FLT accumulation in 6 nude mice with C6 rat glioma xenografts. Accumulation values represent %ID/g values from ROI analysis of tumor xenografts from microPET images.

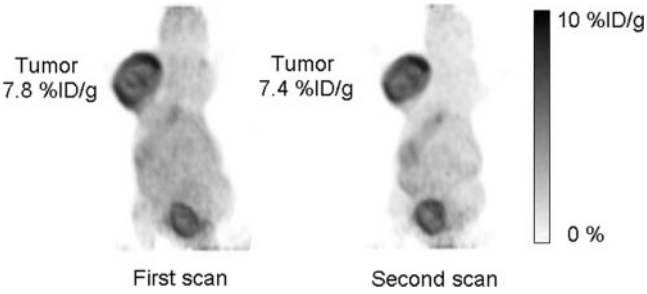

FIGURE 3. 3D volume renderings of nude mouse C6 tumor xenograft scans showing reproducibility of ^{18}F-FLT microPET. (Left) First scan. (Right) Second scan obtained 6 h later, after second injection of ^{18}F-FLT. Mean %ID/g values are shown adjacent to tumor xenografts.

is in contrast to findings in human studies, in which bone marrow activity is extremely intense at 1 h.

Reproducibility of ^{18}F-FLT microPET Studies

CVs, differences between the first and second scans, and intraclass correlation coefficients were calculated to determine the reproducibility of the mean ROI %ID/g measurement (Table 1). The CV between the first and second scans for the mean %ID/g was 14% ± 10%. The CV for the mean SUV was similar (15% ± 10%), because the body weights for all of the mice were very similar (mean ± SD, 25.1 ± 2.2 g). The CVs for the maximum %ID/g and the maximum SUV were higher (35% ± 24% and 35% ± 24%, respectively).

The difference in the mean %ID/g activity between scans across all 17 mice was −0.06% ± 1.3% (not statistically different from 0). The difference in the mean SUV between scans was −0.05% ± 0.34%. The differences in the maximum %ID/g activity and the maximum SUV between scans were larger (−0.04% ± 5.9% and −0.16% ± 1.5%, respectively). The intraclass correlation coefficients for the mean %ID/g, mean SUV, maximum %ID/g, and maximum SUV were 0.60, 0.56, 0.45, and 0.43, respectively.

Three studies were excluded because the mouse temperature was 24°C on the initial scan because the heating pad was not turned on. These animals did undergo both a first scan at 24°C and a second scan 6 h later at 35°C, a process that revealed an interesting temperature dependence for ^{18}F-FLT accumulation (Fig. 5). The mean ± SD %ID/g tumor activity increased from 3.8% ± 0.6% at 24°C to 7.9% ± 3.6% at 35°C (P = 0.04), a 2-fold increase.

The effects of ROI placement were assessed in several ways. First, the original analyzer redrew ROIs around the tumors in a separate session to allow for possible changes in ROI size and position. The CV for the mean %ID/g between the original and the redrawn ROIs was 6.5% ± 4.7%. There was a close correlation between the CV for the mean %ID/g and the CV for the size of the ROI (R^2 = 0.78). In a second analysis, ROIs of the same sizes were used to assess ROI placement. The CV was much lower—2.3% ± 1.5%. These results suggest that the variability of the mean %ID/g in this analysis was largely a result of the ROI size difference

TABLE 1
Differences Between Scans and CVs in C6 Tumor Xenografts in Nude Mice as Determined from Repeat ^{18}F-FLT microPET Studies

Mouse study	%ID/g for: First scan	%ID/g for: Second scan	Difference	CV (%)
1	4.3	4.4	0.1	1.5
2	5.0	5.2	0.2	3.0
3	7.8	7.4	−0.4	3.3
4	4.9	4.7	−0.2	4.0
5	6.2	6.6	0.4	4.2
6	3.9	4.5	0.6	10
7	4.6	5.3	0.7	10
8	4.4	3.7	−0.7	12
9	4.2	5.1	0.9	14
10	3.3	2.7	−0.6	16
11	5.1	4.0	−1.1	16
12	5.1	6.5	1.4	17
13	5.1	6.6	1.5	17
14	8.0	5.7	−2.3	24
15	6.0	8.6	2.6	25
16	5.6	3.6	−2.0	30
17	4.8	2.7	−2.1	38
Mean ± SD			−0.06 ± 1.3	14 ± 10

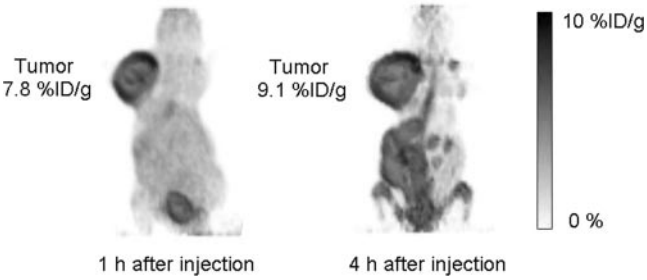

FIGURE 4. 3D volume renderings of nude mouse C6 tumor xenograft scans obtained 1 h (left) and 4 h (right) after single ^{18}F-FLT injection by microPET and showing changes in tumor activity and tracer distribution over time. Mean %ID/g values are shown adjacent to tumor xenografts.

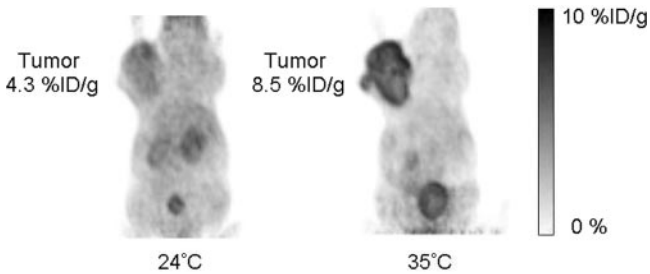

FIGURE 5. 3D volume renderings of nude mouse C6 tumor xenograft scans displaying temperature dependence of ^{18}F-FLT microPET at 2 different temperatures, 24°C (left) and 35°C (right). Mean %ID/g values are shown adjacent to tumor xenografts.

rather than ROI placement. Reanalysis by a second analyzer showed that the CV for the mean %ID/g was 13% ± 7.8% when new ROIs were redrawn but was also much lower—2.2% ± 1.0%—when ROIs of the same sizes were placed.

The accuracy of tail vein injection was assessed by visual inspection of the images. On the 34 scans, a very mild focus of activity was noted in 4 tails (0.5%−1.4% of the injected dose, as determined by ROI analysis), and a moderate focus was seen in 1 tail (9.1% of the injected dose) because of infiltration from a difficult injection. The %ID/g was recalculated by subtracting the tail activity from the injected dose. For the 5 mice evaluated, the recalculated mean %ID/g CV showed only a slight increase, from 8.0% ± 5.9% to 8.3% ± 7.7%.

No significant difference was seen between the mean activity on the first scans and that on the second scans ($P \gg 0.05$). No significant correlations were seen between the tumor activity and the parameters of body weight, injected dose, tumor size, or fasting state ($P \gg 0.05$).

DISCUSSION

We investigated the reproducibility of ^{18}F-FLT microPET scans in nude mouse tumor xenografts and found that the CV for the mean %ID/g was 14% ± 10% and that the average difference between scans was −0.06% ± 1.3%. This finding was seen across a wide range of mean tumor diameters (5–17 mm) and over a range of injected doses (1.9–7.4 MBq [50–200 μCi]).

Because the CV for the %ID/g was 14%, a change in serial studies for a single mouse likely would need to be greater than twice the CV, 28%, to be predictive of a real change. For a group of mice, the cutoff value for a significant change would be lower. These results suggest that serial changes can be reasonably assessed on serial scans because the CV is moderately low, in agreement with a moderate intraclass correlation coefficient of 0.60. Previously, microPET studies that assessed therapy response or drug evaluation did not address the issue of scan reproducibility (*14–17*); however, our results suggest that these types of studies can be performed with a reasonably accurate assessment of serial changes.

Factors Affecting ^{18}F-FLT Accumulation

Compared with human ^{18}F-FDG cancer scans, which had an SUV variability of 6%–10% (*18,19*), our mouse microPET scans had a higher overall variability—14%. We investigated several factors to try to determine the sources of the variability.

First, mouse serum thymidine levels were determined, because in vitro enzyme assays have shown that thymidine and FLT can competitively inhibit the thymidine kinase enzyme (*26*). We showed that thymidine can compete with ^{3}H-FLT in C6 cell cultures (Fig. 1). We then showed that mouse serum thymidine levels have a mild inverse correlation with ^{18}F-FLT microPET %ID/g values (Fig. 2), suggesting that serum thymidine can compete with ^{18}F-FLT in vivo. Minn et al. showed that human ^{18}F-FDG SUV variability was reduced from 10% to 6% by using a correction for serum glucose (*18*). Therefore, adjustment for serum thymidine may reduce the variability in our ^{18}F-FLT microPET studies.

We determined serum thymidine levels in 6 mice at only 1 time point. We would have liked to assess the variability in a single mouse over several days; however, only a limited amount of serum, typically 150 μL over 2 wk, may be obtained from a mouse (*27*). In developing our thymidine assay, we required 50 μL of serum; therefore, in future studies, we will attempt to collect 3 samples in 1 wk to study the variability of thymidine levels in a single mouse over time and to correlate it with the %ID/g. This process will help to further clarify the need for thymidine correction to reduce variability.

Our range of serum thymidine levels varied from 107 to 411 ng/dL, with a mean of 289 ± 107 ng/dL, as determined by our LC-MS/MS assay. This mean is higher than a previously published mean of 166 ng/dL, which was determined by a microbiological *Lactobacillus* growth inhibition assay. In that study (*28*), higher levels were seen in mice with various experimental infections; serum thymidine levels ranged from 63 to 1,021 ng/dL. No signs of infection were seen in the mice throughout our study. Our higher mean may have been attributable to the effect of tumor xenografts on nude mice. An alternative explanation is that because the *Lactobacillus* growth inhibition assay is an indirect assay, it may underestimate the actual amount of thymidine found in the samples. Our use of internal standards reduced the risk of interday and intraday errors that may be present in assays without these controls.

An alternative method for evaluating serum thymidine levels was reported by van Waarde et al. (*29*). They were initially unable to visualize ^{18}F-FLT accumulation in C6 tumor xenografts in rats unless thymidine phosphorylase was injected to reduce endogenous thymidine levels. Pretreatment with thymidine phosphorylase allowed the visualization of tumors with ^{18}F-FLT and reduced the serum thymidine level in 1 rat from 150 ng/mL to undetectable, as measured by a reverse-phase high-performance liquid chromatography assay.

Second, ^{18}F-FLT accumulation in the tumors changed over time. Some tumors showed an increase in %ID/g values over time, whereas others showed a decrease. The change in the tumor time–activity curve has been well characterized in ^{18}F-FDG studies, such that if measurements cannot be performed at the same time, correction factors may be applied to adjust for the time difference (*30*). Our data suggest that in the assessment of serial scans, the time of imaging after injection should remain constant, because %ID/g values vary over time.

Third, large body temperature changes resulted in large changes in %ID/g values (Fig. 5). Mice at 24°C had much less activity than mice at 35°C, probably because of decreased blood flow and decreased body functions at the

lower temperature, which would decrease tracer delivery and cell proliferation. This variation necessitates that the body temperature be regulated with a heating pad or a heat lamp.

Fourth, the size and placement of ROIs can contribute to variability (*31*). Different analyzers may draw ROIs of different sizes on the same tumors. In our analysis, the CVs varied as much as 6% and 13%, largely because of the ROI size difference. When ROIs of the same sizes were used, the CV was reduced to 2.3%. We recommend that ROIs of the same sizes be used for the assessment of serial studies, if possible. Automated methods for ROI drawing also may reduce variability and will be investigated in future studies.

Finally, several variables did not have a significant impact on the %ID/g measurements. Several mice had a small focus of activity in the tail because of difficult injections, but the activity of this focus was usually much lower than 10% of the injected dose. This activity did not cause a significant change in the overall mean %ID/g. Factors such as tumor size, mouse body weight, injected dose (range of 1.9–7.4 MBq [50–200 μCi]), and fasting state did not show significant correlations with the mean %ID/g.

Limitations

We chose to analyze mice with the simple parameter %ID/g to provide evidence that rapid scanning with a simple quantitative analysis can be achieved. More rigorous quantitation of ^{18}F-FLT with compartment modeling or Patlak graphical analysis has been performed (*32–34*) in dog and human studies, but such analyses require a blood input function and longer dynamic scanning, requirements that add time and complexity to the scans. Dynamic studies have been performed with ^{18}F-FDG microPET to help develop protocols for mouse studies (*35,36*). Despite more rigorous quantitation, compartment modeling and Patlak analysis did not significantly reduce the variability in human tumor ^{18}F-FDG PET scans (*18,19*); however, these techniques will be explored in future studies to assess for improved quantitation in mouse microPET studies, because there may be technical differences between mouse and human studies. It is possible that the blood time–activity curve, if available, would help reduce variability by allowing the use of the area under the curve instead of the injected dose to normalize for uptake. Future studies will attempt to study reductions in variability with the trade-off of the use of the blood time–activity curve obtained through more technically demanding procedures. Visvikis et al. showed that the ^{18}F-FLT SUV in human oncology studies had a good correlation ($R^2 = 0.85$) with Patlak analysis or K_i (*34*), suggesting that the simpler parameter %ID/g may suffice for rapid drug screening or therapy monitoring if sample sizes are large enough to offset the variability characterized in this work. However, in mice, in which it is much more difficult to inject a tracer via the tail vein, the blood time–activity curve may be more variable.

Attenuation correction was not performed in the mice that we studied because attenuation for mice is fairly small (*37*). We found that using uniform attenuation correction did not significantly alter the activity profile across mice and therefore likely would not affect the variability of serial scans. Ongoing studies are being performed to further assess the need for attenuation correction with transmission scans.

The CV was calculated from only 2 data points for each mouse, namely, the first scan and the second scan. Ideally, several studies would be performed to calculate the CV, but given the limited availability of ^{18}F-FLT and the daily increase in tumor volumes, which could change tumor activity, we were unable to perform more than 2 studies. We attempted to circumvent studying a single mouse several times by studying a larger number of mice.

Because we performed 2 ^{18}F-FLT studies within 6 h, the second scan had a small amount of residual activity from the first scan; therefore, assessment of the difference between the scans was dependent on the accuracy of the technique used to subtract the activity of the first scan from that of the second scan. For our analysis, the activity from the first scan was assumed to decay exponentially over time without regard to changes in activity attributable to biologic changes over the 6 h between the first scan and the second scan; however, some tumors may show an increase in activity over time, whereas others may show a decrease. One method for improving the subtraction technique would be to obtain a delayed scan immediately before the second injection and then subtract the activity seen in the delayed scan. However, this method would introduce a new variable, because the mice would undergo an additional exposure to anesthesia during the delayed scan, which could affect variability.

To assess the contribution of this variable, a subanalysis was performed on 4 mice that underwent a delayed scan 4 h after the first injection and then had a subsequent second injection and scan. The mean %ID/g for the tumor increased in 2 mice and decreased in the other 2 mice at the 4-h time point. The tumor activity in the delayed scan was subtracted from the tumor activity in the scan obtained after the second injection. When this analysis was performed, the CVs for these 4 mice improved from 9.2% ± 6.7% to 4.9% ± 5.4% ($P = 0.10$). When the 4 recalculated CVs were combined with the CVs from the remaining 13 studies, the overall CV was reduced slightly, from 14% ± 10% to 13% ± 11%. These results suggest that the 14% CV likely represents an upper bound and may be reduced by use of a delayed scan. Overall, the subtraction technique was a small source of variability and would be a factor only if scans were performed within short time intervals, when there would be residual activity from an earlier injection.

The ability to generalize the findings of this work to other tumor types studied with ^{18}F-FLT and microPET also will be important. Although it would be unusual for the findings to be tumor type dependent, if a given tumor has much lower ^{18}F-FLT uptake than other C6 tumors, then serial study variability may be increased. In addition, it will be important to understand how the results can be generalized

to other tracers (e.g., ^{18}F-FDG) with a tumor xenograft model and microPET imaging.

CONCLUSION

^{18}F-FLT microPET mouse tumor xenograft studies are reproducible with moderately low variability. Strict attention to consistent protocol parameters, in particular, temperature, time of imaging after injection, and ROI definition, can ensure accurate repeat scans. Serum thymidine can compete with ^{18}F-FLT, and adjustment should be considered for accurate quantitation. Overall, serial studies may be performed to assess changes for preclinical drug screening or therapy response studies with reasonably low thresholds for significant changes.

ACKNOWLEDGMENTS

Many thanks are extended to the members of Dr. Sanjiv S. Gambhir's laboratory, including Dr. Shay Keren, for assistance with microPET imaging, Dr. Pritha Ray, for assistance with cell culture techniques, and Andreas Loening, for assistance with image processing. Appreciation is extended to Dr. Anthony Shields for helpful discussions. Financial support was provided by NIH In Vivo Cellular and Molecular Imaging Center grant (ICMIC grant P50CA114747). This work was funded in part through the NCI Small Animal Imaging Resource Program (SAIRP grant R24CA92862).

REFERENCES

1. Shields AF, Grierson JR, Dohmen BM, et al. Imaging proliferation in vivo with [F-18]FLT and positron emission tomography. *Nat Med*. 1998;4:1334–1336.
2. Rasey JS, Grierson JR, Wiens LW, Kolb PD, Schwartz JL. Validation of FLT uptake as a measure of thymidine kinase-1 activity in A549 carcinoma cells. *J Nucl Med*. 2002;43:1210–1217.
3. Seitz U, Wagner M, Neumaier B, et al. Evaluation of pyrimidine metabolising enzymes and in vitro uptake of 3′-[^{18}F]fluoro-3′-deoxythymidine ([^{18}F]FLT) in pancreatic cancer cell lines. *Eur J Nucl Med Mol Imaging*. 2002;29:1174–1181.
4. Toyohara J, Waki A, Takamatsu S, et al. Basis of FLT as a cell proliferation marker: comparative uptake studies with [^{3}H]thymidine and [^{3}H]arabinothymidine, and cell-analysis in 22 asynchronously growing tumor cell lines. *Nucl Med Biol*. 2002;29:281–287.
5. Schwartz JL, Tamura Y, Jordan R, Grierson JR, Krohn KA. Monitoring tumor cell proliferation by targeting DNA synthetic processes with thymidine and thymidine analogs. *J Nucl Med*. 2003;44:2027–2032.
6. Buck AK, Schirrmeister H, Hetzel M, et al. 3-Deoxy-3-[^{18}F]fluorothymidine-positron emission tomography for noninvasive assessment of proliferation in pulmonary nodules. *Cancer Res*. 2002;62:3331–3334.
7. Vesselle H, Grierson J, Muzi M, et al. In vivo validation of 3′deoxy-3′-[^{18}F]fluorothymidine ([^{18}F]FLT) as a proliferation imaging tracer in humans: correlation of [^{18}F]FLT uptake by positron emission tomography with Ki-67 immunohistochemistry and flow cytometry in human lung tumors. *Clin Cancer Res*. 2002;8:3315–3323.
8. Dittmann H, Dohmen BM, Paulsen F, et al. [^{18}F]FLT PET for diagnosis and staging of thoracic tumours. *Eur J Nucl Med Mol Imaging*. 2003;30:1407–1412.
9. Francis DL, Visvikis D, Costa DC, et al. Potential impact of [^{18}F]3′-deoxy-3′-fluorothymidine versus [^{18}F]fluoro-2-deoxy-D-glucose in positron emission tomography for colorectal cancer. *Eur J Nucl Med Mol Imaging*. 2003;30:988–994.
10. Smyczek-Gargya B, Fersis N, Dittmann H, et al. PET with [^{18}F]fluorothymidine for imaging of primary breast cancer: a pilot study. *Eur J Nucl Med Mol Imaging*. 2004;31:720–724.
11. Cobben DC, Jager PL, Elsinga PH, et al. 3′-^{18}F-Fluoro-3′-deoxy-L-thymidine: a new tracer for staging metastatic melanoma? *J Nucl Med*. 2003;44:1927–1932.
12. Cobben DC, Elsinga PH, Suurmeijer AJ, et al. Detection and grading of soft tissue sarcomas of the extremities with ^{18}F-3′-fluoro-3′-deoxy-L-thymidine. *Clin Cancer Res*. 2004;10:1685–1690.
13. Buchmann I, Neumaier B, Schreckenberger M, Reske S. [^{18}F]3′-Deoxy-3′-fluorothymidine-PET in NHL patients: whole-body biodistribution and imaging of lymphoma manifestations—a pilot study. *Cancer Biother Radiopharm*. 2004;19:436–442.
14. Barthel H, Cleij MC, Collingridge DR, et al. 3′-Deoxy-3′-[^{18}F]fluorothymidine as a new marker for monitoring tumor response to antiproliferative therapy in vivo with positron emission tomography. *Cancer Res*. 2003;63:3791–3798.
15. Sugiyama M, Sakahara H, Sato K, et al. Evaluation of 3′-deoxy-3′-^{18}F-fluorothymidine for monitoring tumor response to radiotherapy and photodynamic therapy in mice. *J Nucl Med*. 2004;45:1754–1758.
16. Oyama N, Ponde DE, Dence C, et al. Monitoring of therapy in androgen-dependent prostate tumor model by measuring tumor proliferation. *J Nucl Med*. 2004;45:519–525.
17. Waldherr C, Mellinghoff IK, Tran C, et al. Monitoring antiproliferative responses to kinase inhibitor therapy in mice with 3′-deoxy-3′-^{18}F-fluorothymidine PET. *J Nucl Med*. 2005;46:114–120.
18. Minn H, Zasadny KR, Quint LE, Wahl RL. Lung cancer: reproducibility of quantitative measurements for evaluating 2-[F-18]-fluoro-2-deoxy-D-glucose uptake at PET. *Radiology*. 1995;196:167–173.
19. Weber WA, Ziegler SI, Thodtmann R, Hanauske AR, Schwaiger M. Reproducibility of metabolic measurements in malignant tumors using FDG PET. *J Nucl Med*. 1999;40:1771–1777.
20. Grierson JR, Shields AF. Radiosynthesis of 3′-deoxy-3′-[^{18}F]fluorothymidine: [^{18}F]FLT for imaging of cellular proliferation in vivo. *Nucl Med Biol*. 2000;27:143–156.
21. Hoffman EJ, Huang SC, Phelps ME. Quantitation in positron emission computed tomography. 1. Effect of object size. *J Comput Assist Tomogr*. 1979;3:299–308.
22. Knoess C, Siegel S, Smith A, et al. Performance evaluation of the microPET R4 PET scanner for rodents. *Eur J Nucl Med Mol Imaging*. 2003;30:737–747.
23. Hudson HM, Larkin RS. Accelerated image reconstruction using ordered subsets of projection data. *IEEE Trans Med Imaging*. 1994;13:601–609.
24. Loening AM, Gambhir SS. AMIDE: a free software tool for multimodality medical image analysis. *Mol Imaging*. 2003;2:131–137.
25. Atkinson G, Nevill AM. Statistical methods for assessing measurement error (reliability) in variables relevant to sports medicine. *Sports Med*. 1998;26:217–238.
26. Munch-Petersen B, Cloos L, Tyrsted G, Eriksson S. Diverging substrate specificity of pure human thymidine kinases 1 and 2 against antiviral dideoxynucleosides. *J Biol Chem*. 1991;266:9032–9038.
27. Hoff J. Methods of blood collection in the mouse. *Lab Animal*. 2000;29:47–53.
28. Nottebrock H, Then R. Thymidine concentrations in serum and urine of different animal species and man. *Biochem Pharmacol*. 1977;26:2175–2179.
29. van Waarde A, Cobben DC, Suurmeijer AJ, et al. Selectivity of ^{18}F-FLT and ^{18}F-FDG for differentiating tumor from inflammation in a rodent model. *J Nucl Med*. 2004;45:695–700.
30. Beaulieu S, Kinahan P, Tseng J, et al. SUV varies with time after injection in ^{18}F-FDG PET of breast cancer: characterization and method to adjust for time differences. *J Nucl Med*. 2003;44:1044–1050.
31. Krak NC, Boellaard R, Hoekstra OS, et al. Effects of ROI definition and reconstruction method on quantitative outcome and applicability in a response monitoring trial. *Eur J Nucl Med Mol Imaging*. 2005;32:294–301.
32. Shields AF, Grierson JR, Muzik O, et al. Kinetics of 3′-deoxy-3′-[F-18]fluorothymidine uptake and retention in dogs. *Mol Imaging Biol*. 2002;4:83–89.
33. Muzi M, Mankoff DA, Grierson JR, et al. Kinetic modeling of 3′-deoxy-3′-fluorothymidine in somatic tumors: mathematical studies. *J Nucl Med*. 2005;46:371–380.
34. Visvikis D, Francis D, Mulligan R, et al. Comparison of methodologies for the in vivo assessment of 18FLT utilisation in colorectal cancer. *Eur J Nucl Med Mol Imaging*. 2004;31:169–178.
35. Green LA, Gambhir SS, Srinivasan A, et al. Noninvasive methods for quantitating blood time–activity curves from mouse PET images obtained with fluorine-18-fluorodeoxyglucose. *J Nucl Med*. 1998;39:729–734.
36. Huang SC, Wu HM, Shoghi-Jadid K, et al. Investigation of a new input function validation approach for dynamic mouse microPET studies. *Mol Imaging Biol*. 2004;6:34–46.
37. Tai YC, Ruangma A, Rowland D, et al. Performance evaluation of the microPET Focus: a third-generation microPET scanner dedicated to animal imaging. *J Nucl Med*. 2005;46:455–463.

JNM The Journal of NUCLEAR MEDICINE

Reproducibility of 3′-Deoxy-3′-^{18}F-Fluorothymidine MicroPET Studies in Tumor Xenografts in Mice

Jeffrey R. Tseng, Mangal Dandekar, Murugesan Subbarayan, Zhen Cheng, Jinha M. Park, Stan Louie and Sanjiv S. Gambhir

J Nucl Med. 2005;46:1851-1857.

The Journal of Nuclear Medicine is published monthly.
SNMMI | Society of Nuclear Medicine and Molecular Imaging
1850 Samuel Morse Drive, Reston, VA 20190.
(Print ISSN: 0161-5505, Online ISSN: 2159-662X)

SNMMI SOCIETY OF NUCLEAR MEDICINE AND MOLECULAR IMAGING